ELSEVIER

Chemical Engineering Journal 137 (2008) 189–197

Chemical Engineering Journal

www.elsevier.com/locate/cej

Sensitivity analysis and faults diagnosis using artificial neural networks in natural gas TEG-dehydration plants

Naif A. Darwish [a,*], Nidal Hilal [b]

[a] *Department of Chemical Engineering, The Petroleum Institute, P.O. Box 2533, Abu Dhabi, United Arab Emirates*

[b] *Centre for Clean Water Technologies, School of Chemical, Environmental and Mining Engineering, The University of Nottingham, NG7 2RD, United Kingdom*

Received 27 September 2006; received in revised form 26 March 2007; accepted 1 April 2007

Abstract

In this work, a typical process for natural gas dehydration using triethylene glycol (TEG) as a desiccant is simulated using a steady state flowsheet simulator (Aspen Plus). The flowsheet includes all major units in a typical dehydration facility, that is: absorption column, flash unit, heat exchangers, regenerator, stripper, and reboiler. The base case operating conditions are taken to resemble field data from one of the existing TEG-dehydration units operating in United Arab Emirates (UAE). Using Aspen Plus, the flowsheet is then used to study the effects of different input parameters and operating conditions of the absorption column, the stripper and the overall plant, on BTEX emission, volatile organic components (VOCs) emission, TEG losses and water content (dew point) of the dehumidified natural gas. Contactor performance has been found to be most sensitive to disturbances in operating pressure and wet gas flow rate, whereas flow rate of stripping gas and temperature of inlet solvent have the major impact on the stripper performance. The potential of artificial neural network (ANN) to detect and diagnose process faults in the dehydration plant has also been explored. ANN successfully detects the disturbance severity levels in the input variables considered for the contactor. In particular, abnormal levels of BTEX concentrations in the rich solvent (exiting the contactor) are shown to precisely indicate the severity levels in the input variables. Faults in the stripper–regenerator unit have been perfectly predicted by the ANN for two symptoms (TEG emissions and BTEX emissions in vents) and to a lesser extent for faults in VOCs emissions. The best ANN prediction is obtained for the overall plant where the ANN simulates the imposed disturbances for three severity levels of imposed malfunctions for all symptoms considered.

Keywords: Natural gas; Dehydration; Emission; BTEX; Simulation; Mixing rules; Equations of state

1. Introduction

1.1. BTEX and VOCs emissions

Gas dehydration is one of the most prominent unit operations in the natural gas industry. In this operation water vapor (moisture) is removed from natural gas streams to meet sales specifications or other downstream gas processes such as gas liquid recovery. In particular, moisture level in natural gas must be maintained below a certain threshold so as to prevent hydrate formation and minimize corrosion in transmission pipelines [1–4]. The most widely used dehydration processes involve the removal of water vapor by absorption into a liquid desiccant (e.g., glycol) in an absorber (also called contactor). To maintain continuity of the process, the water-laden (rich) solvent must be regenerated to recover the desiccant in a still column (stripper). The medium used to strip water vapor from the rich solvent in the stripper is usually steam and/or some dry stripping gas like air. The operating conditions favoring efficient operation of the stripper are high temperature and low pressure [3], which are opposite to the conditions required in the absorber. The flowsheet for a typical natural gas dehydration facility (the one that has been simulated here) is shown in Fig. 1. This flowsheet represents a typical glycol dehydration unit and resembles many of the dehydration units in current use (e.g., ADCO dehydration facility in the United Arab Emirates). Details of the base-case operating conditions in this facility have been presented elsewhere [5]. The rich desiccant leaving the bottom of the absorber is throttled in a flash tank to a lower pressure before being sent to the strip-

* Corresponding author. Tel.: +971 2 5085455.
E-mail addresses: ndarwish@pi.ac.ae (N.A. Darwish), Nidal.Hilal@nottingham.ac.uk (N. Hilal).

1385-8947/$ – see front matter © 2007 Elsevier B.V. All rights reserved.
doi:10.1016/j.cej.2007.04.008

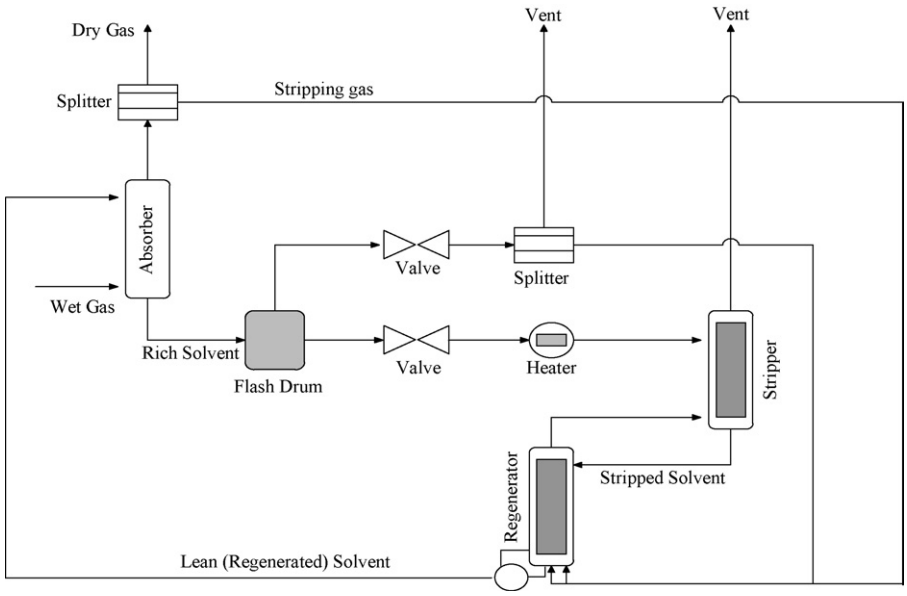

Fig. 1. Process flowsheet for the simulated natural gas dehydration plant.

per/regenerator unit, where the absorbed species are stripped off the solvent. The major source of air and water pollution in dehydration units is associated with the vent gases from this stripper [4,5].

Unfortunately, in liquid-desiccant–dehydration-processes significant amounts of Benzene, Toluene, Ethyl-benzene, and Xylenes (BTEX) and volatile organic compounds (VOCs), entering with the wet gas, are simultaneously absorbed. Upon regeneration of the liquid desiccant in the stripper–regenerator system, BTEX and VOCs are rejected in the vents [6,7]. Water recovered from the rich solvent may also contain significant amounts of these objectionable materials [8,9]. Because of the growing stringency of environmental regulations, attention has been increasingly focused on emissions associated with glycol dehydration units [10–12]. Currently, the limits placed by the "Clean Air Amendments" on BTEX emissions are 25 tonnes per year (tpy) of total BTEX and no more than 10 tpy of any individual compound [13]. Control of BTEX and other VOCs emissions from gas and oil facilities is becoming, therefore, one of the largest environmental challenges facing the natural gas industry today [13]. The two most common emission control technologies in current use are combustion (sometimes called flaring or incineration) and condensation [14].

Optimization of process parameters, such as glycol circulation rate, temperature and pressure, can reduce pollutant emissions from glycol dehydration facilities. However, some dehydrators, even under optimum operating conditions, may generate emissions above regulatory limits [5,15,16]. The choice of desiccant (absorbing solvent) in a certain dehydration plant crucially affects the resulting pollution problem. Ideally, a solvent that selectively absorbs water but not other hydrocarbons is required. Absorbing BTEX and other VOCs, besides water, will pose a serious environmental problem in a later stage upon regeneration.

1.2. Fault diagnosis using artificial neural networks (ANNs)

ANNs are extensively interconnected parallel structures composed of consecutive layers of processing elements called neurons. In a feed-forward network each neuron forms weighted connections to all neurons in the subsequent layer. ANNs interface independent variables through the neurons of an input layer and transmit output of dependent variables through the neurons of an output layer. The number of independent variables and the number of dependent variables, therefore, dictates number of neurons in the input and the output layers, respectively. In between the input and the output layers there is at least one hidden layer that can have any number of neurons. The input layer acts as a distribution station by transmitting its input to the neurons of the hidden layer. Neurons in the hidden and the output layers calculate their inputs by performing a weighted sum of the outputs they receive from the previous layer. Their outputs, on the other hand, are calculated by transforming their inputs using a non-linear transfer function. The most widely used transfer functions are the S-shaped log-sigmoid transfer functions (logsig), the S-shaped tan-sigmoid transfer functions (tansig), and the pure linear transfer function (purelin). The logsig transfer function produces outputs in the range of 0–1, whereas the tansig function produces output in the range of −1 to +1. Outputs in any range can be produced by the purelin transfer function [17–20]. The architecture of the general ANN with a single hidden layer is shown in Fig. 2.

ANNs are categorized as black-box models that can handle multidimensional problems of high degree of nonlinearity and inter-dependence. The principle utilized by ANNs is that a system of highly interconnected simple processing elements can learn complex interrelationships between independent and dependent variables. ANNs have found many applications in different fields of chemical engineering [21,18,19].

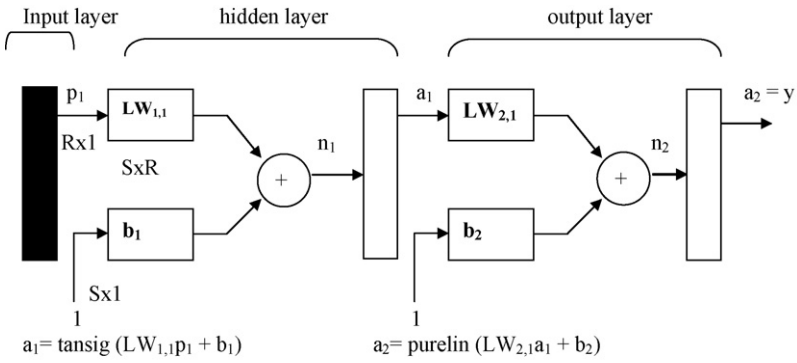

Fig. 2. Architecture of a general neural network with one hidden layer.

Usually, there are four steps involved in ANN modeling: (1) assembling the training data of input (independent variables) and output (dependent variables), (2) deciding the network architecture, (3) training the network, and (4) simulating the network response to new inputs. The training process is simply an optimization process which aims at finding the set of weight and biases associated with each layer that will minimize the error objective function related to the deviations of the network predictions from the true response output data of the training set. Recently, there has been a growing interest in the application of ANN in fault diagnosis, pattern recognition and adaptive nonlinear control of chemical processes [22–32].

In the first part of this work, a typical natural gas TEG-dehydration facility is simulated using a flowsheet simulator (Aspen Plus). All major units are included in the flowsheet, that is: absorption column, flash unit, heat exchangers, regenerator, stripper, and reboiler. The base case operating conditions are taken to resemble field data from one of the existing dehydration units operating in the United Arab Emirates (UAE). Using Aspen Plus simulator as a modeling tool, the sensitivity of selected responses (output variables) in the contactor, the stripper, and the overall plant towards disturbances in the range of −20% to +20% in the major input variables in these units are investigated. In a previous study by one of the authors [16], the performance of natural gas glycol dehydration was simulated and the capability of different thermodynamic models in describing the whole process was explored. It was found that Peng-Robinson cubic equation of state with the modified Huron and Vidal (second order approximation) predictive mixing rules (PR-MHV2) gives conservative emission rates of BTEX. Therefore, the same model is selected as the property method in the simulator. This model, in addition to others, has been summarized elsewhere [16].

In the second part of this work the potential of ANNs to diagnose process faults in the performance of the contactor, the stripper, and the overall plant is explored. Process faults considered here cause fluctuations in the plant's performance but not failures or operational hazards that incurs plant shutdown. Following a troubleshooting study to investigate the effects of the number of hidden layers and the number of neurons involved in these hidden layers, a 1-3-1 network, with tansig-purelin transfer functions, was found to be the most optimum in terms of the root mean squared errors (RMSE) obtained. Moreover, one of the training algorithms in the neural networks toolbox in MATLAB, which is based on the regularization principles (i.e., trainbr), has a unique feature of automatically selecting the best architecture of a neural network for a given input–output data. This algorithm also gave the same 1-3-1 structure for the best network.

The data needed in the ANN training phase are generated by Aspen Plus simulator, which has been verified previously to give reliable simulation of the plant under consideration [16]. The input has been normalized to the range of −1 to +1. The backpropagation training algorithms used here fall in two categories: (1) training algorithms based on the quasi-Newton (secant) method, which, in minimizing the error objective function, track the steepest descent direction but do not require calculations of the Hessian matrix, and (2) training algorithms based on the conjugate gradient principles, which, in their search for the minimum, follows a path in the direction of conjugate gradient. Of the first kind, the Broyden-Fletcher-Goldfarb-Shanno algorithm (trainbfg), and the one-step-secant algorithm (trainoss) have been utilized. Of the second type, the Powell-Beale algorithm (traincgb) is used. All algorithms were used as programmed in the neural network toolbox of Matlab 6.0. Some other algorithms, like those based on the regularization principles, have been tried but found to be more sensitive towards the initial guesses of the network weights, which are generated automatically by MATLAB (i.e., higher standard deviations than those appearing in Table 3).

2. Results and discussions

The base case operating conditions in the different units, and the composition of the inlet wet gas, which are used in the current simulation have been presented elsewhere [16] and reproduced here in Table 1 for convenience. These conditions resemble one of the onshore oil and gas-processing facilities in the United Arab Emirates (UAE), which is operated by Abu Dhabi Company for Onshore Oil Operations (ADCO) [5]. These conditions are based on field sampling tests that are slightly different from field sampling presented before [5]. The flowsheet representing this process is reproduced in Fig. 1. As shown in this figure, all major units are taken into consideration, that is: the absorption column, flash unit, heat exchangers, stripper, regenerator, and reboiler.

Table 1
Summary of operating conditions of the base case employed in the simulation

Stream or unit	Operating conditions
(1) Wet gas	Temperature = 136.4 °F, pressure = 618 psia, volume flow = 11 MMSCFD, mass flow = 31915 lb/h
(2) Lean TEG	Temperature = 148 °F, pressure = 618 psia, purity = 0.998, circulation rate = 9.25 gpm
(3) Stripping gas	80% of the flash tank vent
(4) Absorber	Number of ideal stages = 3, pressure = 618 psia, simulator input: no reboiler ($Q_N = 0$), no condenser ($Q_1 = 0$)
(5) Flash tank	Temperature = 100 °F, pressure = 58 psia
(6) Stripper	Number of ideal stages = 5, pressure = 14.7 psia, simulator input: no reboiler ($Q_N = 0$), no condenser ($Q_1 = 0$)
(7) Regenerator	Number of ideal stages = 2, pressure = 1.7 psia, simulator input: no condenser ($Q_1 = 0$), heat duty controlled to give lean solvent temperature of 400 °F (field value is 0.6 MMBtu/h)

2.1. Sensitivity analysis

In this part Aspen Plus simulator is used for the investigation of the sensitivity of selected responses (output variables) in the contactor, the stripper, and the overall plant towards disturbances (in the range of −20% to +20% of the base case values) in the major input variables of these units. In a previous work [5,16], the reliability of the results obtained from Aspen Plus and HYSYS flowsheet simulators in describing the steady state behavior of the TEG dehydration plant considered in this study has been established. The input variables and the response variables selected are displayed in Table 2. For every level of sensitivity studied, the simulator is run with the input variable under study disturbed by the required level keeping all other variables at their base conditions. Results thus obtained, converted to percentages of the values that would have been obtained from the undisturbed base case, are displayed in Figs. 3–5. The consistency of the sensitivity study is evident in each of these figures, where plots for the different input variables pass through the same zero%-disturbance point (i.e., all pass through the base case point).

Table 2
Input and output variables used in the sensitivity analysis study for the contactor, the stripper, and the overall plant

Independent (input) variables	Dependent (output, response) variables
Contactor	
Lean solvent circulation rate	Water contents in dried gas
Lean solvent purity (mass fraction)	TEG losses in dried gas
Lean solvent temperature	BTEX absorbed in rich solvent
Wet gas flow rate	
Water contents in wet gas	
Contactor pressure	
Stripper–regenerator	
Reboiler duty	TEG losses in stripper's vent
Temperature of rich incoming solvent	BTEX emitted in stripper's vent
Flow rate of stripping gas	VOCs emitted in stripper's vent
Overall plants	
Lean solvent circulation rate	TEG losses in stripper's vent
Lean solvent temperature	BTEX emitted in stripper's vent
Contactor pressure	VOCs emitted in stripper's vent

The effects of disturbances in the six input variables selected for the contactor (Table 2) on the amount of water content and the desiccant losses in the dry gas are presented in Fig. 3A and B, respectively. Water contents in the processed dry gas is most sensitive to the wet gas flow rate, where it is seen that in going from 80% to 120% of the base case flow rate, which is 11 MMSCFD [16], water contents increases from 72% to 130%. Lean solvent circulation rate and the amount of water in the inlet wet gas affect water contents in the dried gas to a lesser extent (Fig. 3A). However, it is well known that solvent circulation rate has a sizeable effect on the water content in the dried gas. It is quite possible that the circulation rate employed in the simulator (and the actual plant) is very much larger than the required solvent rate. This can render the water content in the processed dry gas insensitive to the imposed levels of disturbances in the circulation rate. The other three input variables affect water contents marginally. As to desiccant losses, only contactor pressure has a sound effect (Fig. 3B); TEG losses monotonically increases from 62% to 160% when contactor pressure sweeps an ascending change from 80% to 120% of the base case value, which is 618 psia. Increasing contactor pressure, while holding fixed volumetric flow rate and temperature, is equivalent to increasing mass or molar flow rate of the gas. For the same contactor, in turn, this means higher superficial velocity of the ascending gas in the contactor resulting in higher carry over of the solvent. Lean solvent circulation rate and water contents of the inlet gas have almost no effect on solvent losses. The other three input variables have marginal effects on TEG losses.

The effects of the three input variables of the stripper–regenerator unit on both BTEX and VOCs emissions are displayed in Fig. 4A and B, respectively. Reboiler heat duty and flow rate of the stripping gas are shown to be only slightly affecting BTEX emissions (Fig. 4A). For example, BTEX emission remains in the range of 93–105% when both of these input variables increased from 80% to 120% of their base case values. The temperature of the inlet rich solvent, however, drastically affects BTEX emission, where it is seen

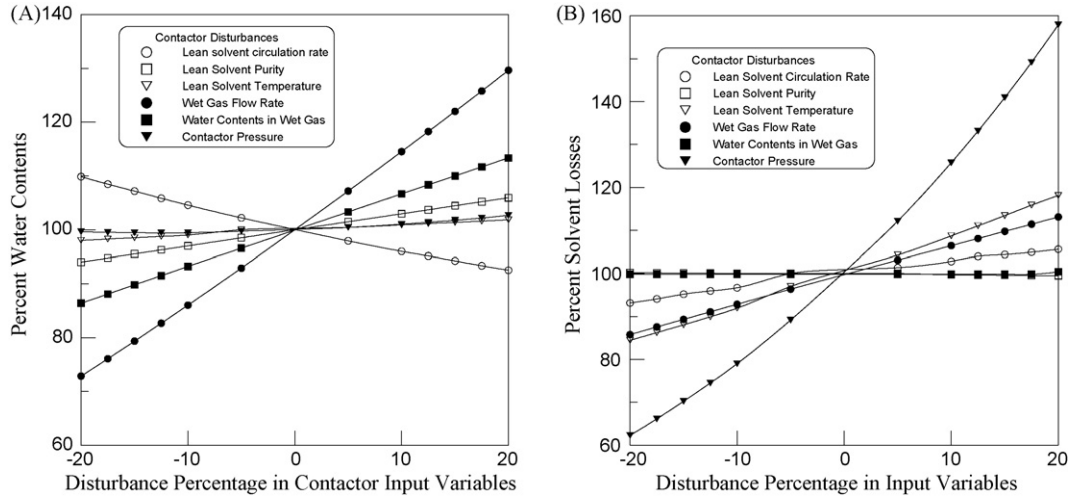

Fig. 3. Sensitivity of water contents (A) and solvent losses (B) in the dry gas towards disturbances in different input parameters of the contactor.

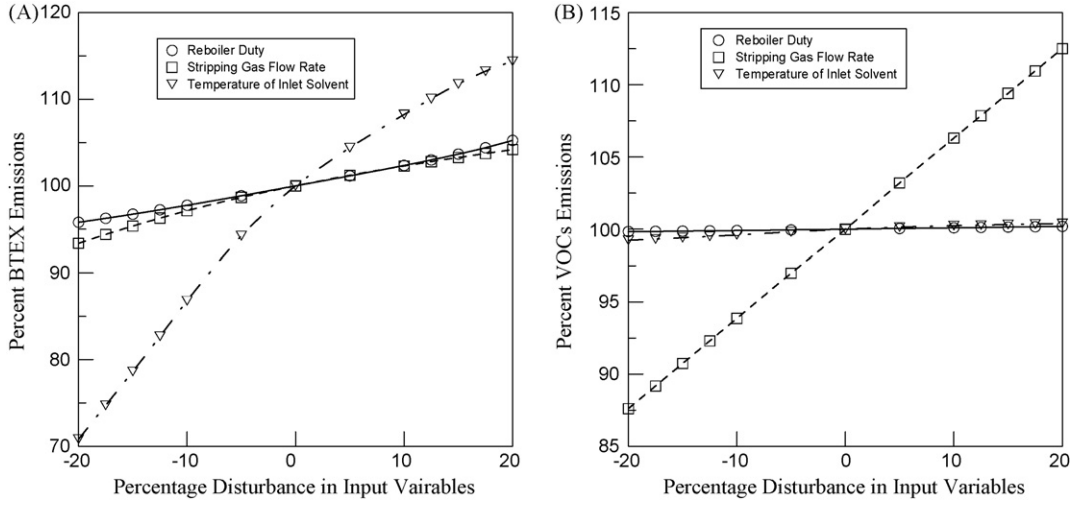

Fig. 4. Sensitivity of BTEX (A) and VOCs emissions (B) towards disturbances in different input parameters of the stripper–regenerator unit.

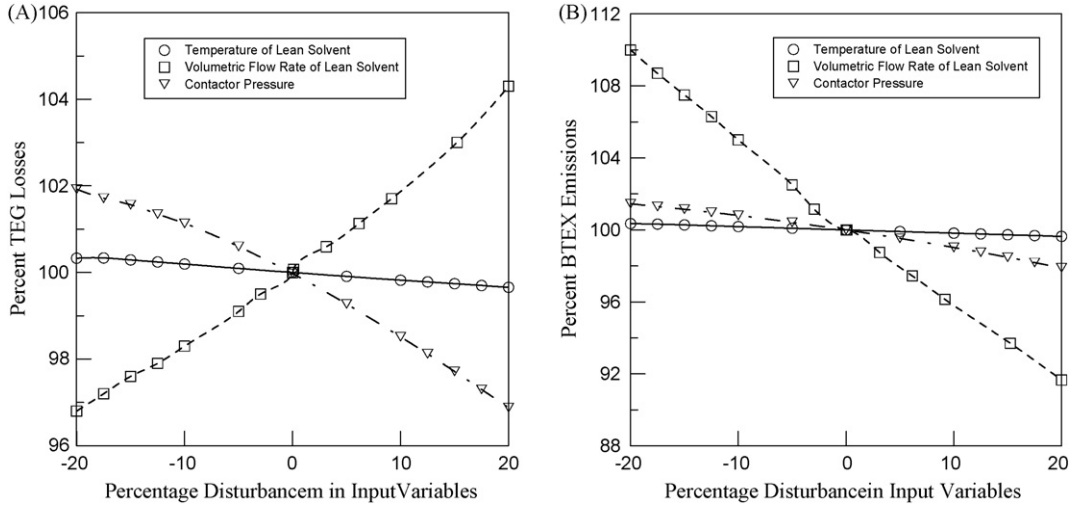

Fig. 5. Sensitivity of solvent losses (A) and BTEX emissions (B) in the stripper's vent towards disturbances in lean solvent temperature, lean solvent volumetric flow rate and contactor pressure.

from Fig. 4A that an increase in BTEX emission from 70% to 115% results upon increasing that temperature from 80% to 120% of the base case temperature, which is 140 °F. It is also evident from the same figure that BTEX emission responds faster to changes in rich solvent temperature in the lower region (for disturbances from −20% to 0%) than in the upper region (for disturbances from 0% to 20%). VOCs emissions on the other hand are responding very sluggishly towards disturbances in both reboiler duty and rich solvent inlet temperature, but profoundly to disturbances in the stripping gas flow rate. This is made evident in Fig. 4B, where the VOCs percentage emission traverses in an ascending manner a range from 87% to 115% for disturbances in the stripping gas flow rate ranging from −20% to +20%. One has to keep in mind, however, that the stripping gas used in this simulation is bled from the dry gas output of the contactor, which has a high concentration of VOCs. Stripping using air or nitrogen gas looks more appropriate in view of these results.

Fig. 5A and B presents effects of disturbances in three input variables of the contactor (i.e., solvent temperature, solvent flow rate, and contactor pressure as shown in Table 2) on the TEG losses and BTEX emissions from the stripper. Out of the three independent variables considered, the circulation rate of the lean solvent has the major effect on both solvent losses and BTEX emissions from the stripper. The higher the circulation rate, the higher is the solvent losses and the lower is the BTEX emissions in the stripper vent. However, with increasing solvent flow rate, one would expect an increase in BTEX emissions rather than a decrease. To explain this one has to keep in mind that the BTEX emission considered here is just the amount emitted in the stripper vent. Therefore, with increasing flow rate, more BTEX will be allowed in the lean regenerated solvent for a fixed minimum specification of solvent purity. Overall, however, BTEX emissions from the total plant could increase with the solvent flow rate. In the second place comes the contactor pressure, which inversely affects the solvent (TEG) losses from stripper. Temperature of the lean solvent is seen to be of marginal influence on these two response variables. However, it was shown previously (Fig. 3B) that solvent losses even in the contactor are only moderately sensitive to changes in lean solvent temperature.

2.2. Fault detection using ANNs

The basic objective here is to have an insight as to what malfunctions and what levels of disturbances in these malfunctions are behind abnormal plant symptoms (output), which can be measured online. The malfunctions and symptoms selected for the purpose of this study are, respectively, the independent and dependent parameters presented before in Table 2. The patterns needed for training and testing the ANN are the Aspen-generated results at the prescribed disturbances from −20% to +20% in malfunction variables. All input data are made to span a normalized range from −1 to +1 to suite the transfer function selected for the hidden layer. For all cases, it was found that the net simulation output (testing phase) is dependent on the initial guesses of the weights. The most probable solution was thus obtained by averaging over 100 different trials. The results obtained using three different training algorithms, as programmed in the Neural Network Toolbox of Matlab 6.0 (trainoss, traincgb, and trainbfg) are presented in Tables 3–5. Also, included in these tables are values of standard deviations of the generated 100 observations. In each case, the net was trained using the simulator output at −5%, +5%, −20%, and +20% malfunctions, whereas outputs at −10%, +10%, and +15% were used in the testing phase. This means that, depending on the respective case, the input training matrix (p) involved four times the number of independent variables involved in that case. For example, in the case of the absorber 24 input data points were involved in the training set. ANN simulations were performed with an error goal of 1×10^{-7} and a maximum of 10^3 epochs.

Regarding the contactor performance, the three training algorithms generally over-predict the actual level of malfunctions. This is evident in Table 3, which also shows a good agreement among the three training algorithms. Single malfunctions in each of the independent variables considered for the contactor are successfully detected by the ANN. The net is shown to

Table 3
ANN fault diagnosis for the contactor when the net is trained using three different algorithms on data representing −5%, +5%, −20%, and +20% disturbances for the contactor

Algorithm	Severity		
	−0.5 (−10% Disturbance)	+0.5 (+10% Disturbance)	+0.75 (+15% Disturbance)
Water contents in dry gas			
Trainoss	−0.78 ± 0.019	0.65 ± 0.017	0.86 ± 0.017
Traincgb	−0.71 ± 0.019	0.62 ± 0.020	0.85 ± 0.021
Trainbfg	−0.77 ± 0.022	0.66 ± 0.023	0.87 ± 0.022
Solvent losses			
Trainoss	−0.23 ± 0.024	0.68 ± 0.018	0.82 ± 0.017
Traincgb	−0.02 ± 0.024	0.65 ± 0.021	0.82 ± 0.019
Trainbfg	−0.06 ± 0.025	0.66 ± 0.019	0.85 ± 0.021
BTEX absorbed in rich solvent			
Trainoss	−0.55 ± 0.017	0.50 ± 0.014	0.64 ± 0.022
Traincgb	−0.59 ± 0.019	0.48 ± 0.016	0.61 ± 0.024
Trainbfg	−0.46 ± 0.019	0.48 ± 0.023	0.67 ± 0.025

Table 4
ANN fault diagnosis for the stripper when the net is trained using three different algorithms on data representing −5%, +5%, −20%, and +20% disturbances for the contactor

Algorithm	Severity		
	−0.5 (−10% Disturbance)	+0.5 (+10% Disturbance)	+0.75 (+15% Disturbance)
TEG in stripper's vent			
Trainoss	−0.56 ± 0.022	0.54 ± 0.027	0.76 ± 0.022
Traincgb	−0.55 ± 0.023	0.52 ± 0.028	0.76 ± 0.022
Trainbfg	−0.54 ± 0.025	0.59 ± 0.03	0.77 ± 0.023
BTEX in stripper's vent			
Trainoss	−0.57 ± 0.013	0.56 ± 0.022	0.78 ± 0.016
Traincgb	−0.59 ± 0.015	0.57 ± 0.021	0.80 ± 0.015
Trainbfg	−0.57 ± 0.013	0.61 ± 0.025	0.75 ± 0.016
VOCS (C1–C8) in stripper's vent			
Trainoss	−0.66 ± 0.012	0.77 ± 0.019	0.91 ± 0.009
Traincgb	−0.69 ± 0.015	0.76 ± 0.022	0.91 ± 0.012
Trainbfg	−0.67 ± 0.014	0.75 ± 0.022	0.89 ± 0.012

be able to recognize the faults in all of theses cases. Results in Table 3 that are associated with trainoss algorithm are shown plotted in Fig. 6A. The ideal situation is for all points to coincide with the diagonal line implying that the predicted fault severity matches that imposed one. Most importantly, the best ANN performance is shown in Fig. 6A to be for the amount of BTEX absorbed in the rich solvent. This implies that on-line monitoring of the BTEX concentrations in the rich solvent (exiting the contactor) can reflect the disturbance severity levels in the input variables considered. This is an interesting result in view of the extreme importance of monitoring BTEX levels in the rich solvent, which directly affects BTEX emission levels from later stages.

Table 4 contains results of the ANN fault diagnosis of the stripper–regenerator unit. Except for the last symptom (VOCs emission), the ANN is handling faults in a comparable manner to that in the contactor. Again, the three algorithms give comparable results. For the first two symptoms (TEG emissions and BTEX emissions in vents), the ANN diagnosis of the faults is in good agreement of the imposed fault. Fig. 6B shows results associated with trainoss algorithm, where the previous argument becomes clearer. The symptom that is not as well predicted is the VOCs emission. This could be the case because VOCs emission was found to be sensitive to one independent variable but not for the others (Fig. 4B).

Results presented above (Tables 3 and 4) are for the contactor and the stripper where both malfunctions and symptoms belong to the same piece of equipment. In Table 5, results are presented for the overall plant where malfunctions represent disturbances in some input variables in the plant and symptoms represent responses elsewhere in the plant. The ANN precisely mimics the imposed disturbance level in the input malfunctions considered. This is evident from the close agreement between imposed severity levels (malfunctions) and the ANN predictions (Table 5). The low values of standard deviations in the ANN predictions (remember that ANN output represents an average of 100 trials) point to the robustness of training algorithms and to the minimal effects of initial guesses of weight and biases of the net. This is also made clearer in Fig. 6C which shows a plot of results corresponding to the trainoss algorithm. The ANN reflects the imposed disturbances in the three severity levels of malfunctions.

Table 5
ANN fault diagnosis for the overall plant when the net is trained using three different algorithms on data representing −5%, +5%, −20%, and +20% disturbances for the contactor

Algorithm	Severity		
	−0.5 (−10% Disturbance)	+0.5 (+10% Disturbance)	+0.75 (+15% Disturbance)
TEG in stripper's vent			
Trainoss	−0.59 ± 0.009	0.48 ± 0.010 (0.28–0.71)	0.79 ± 0.009
Traincgb	−0.59 ± 0.010	0.48 ± 0.009	0.80 ± 0.008
Trainbfg	−0.60 ± 0.011	0.49 ± 0.009	0.80 ± 0.008
BTEX in stripper's vent			
Trainoss	−0.53 ± 0.007	0.51 ± 0.007	0.77 ± 0.007
Traincgb	−0.53 ± 0.006	0.50 ± 0.007	0.76 ± 0.008
Trainbfg	−0.53 ± 0.006	0.51 ± 0.007	0.77 ± 0.009
y3: VOCS (C1–C8) in stripper's vent			
Trainoss	−0.53 ± 0.007	0.51 ± 0.006	0.78 ± 0.007
Traincgb	−0.53 ± 0.006	0.50 ± 0.005	0.78 ± 0.007
Trainbfg	−0.53 ± 0.006	0.52 ± 0.006	0.77 ± 0.007

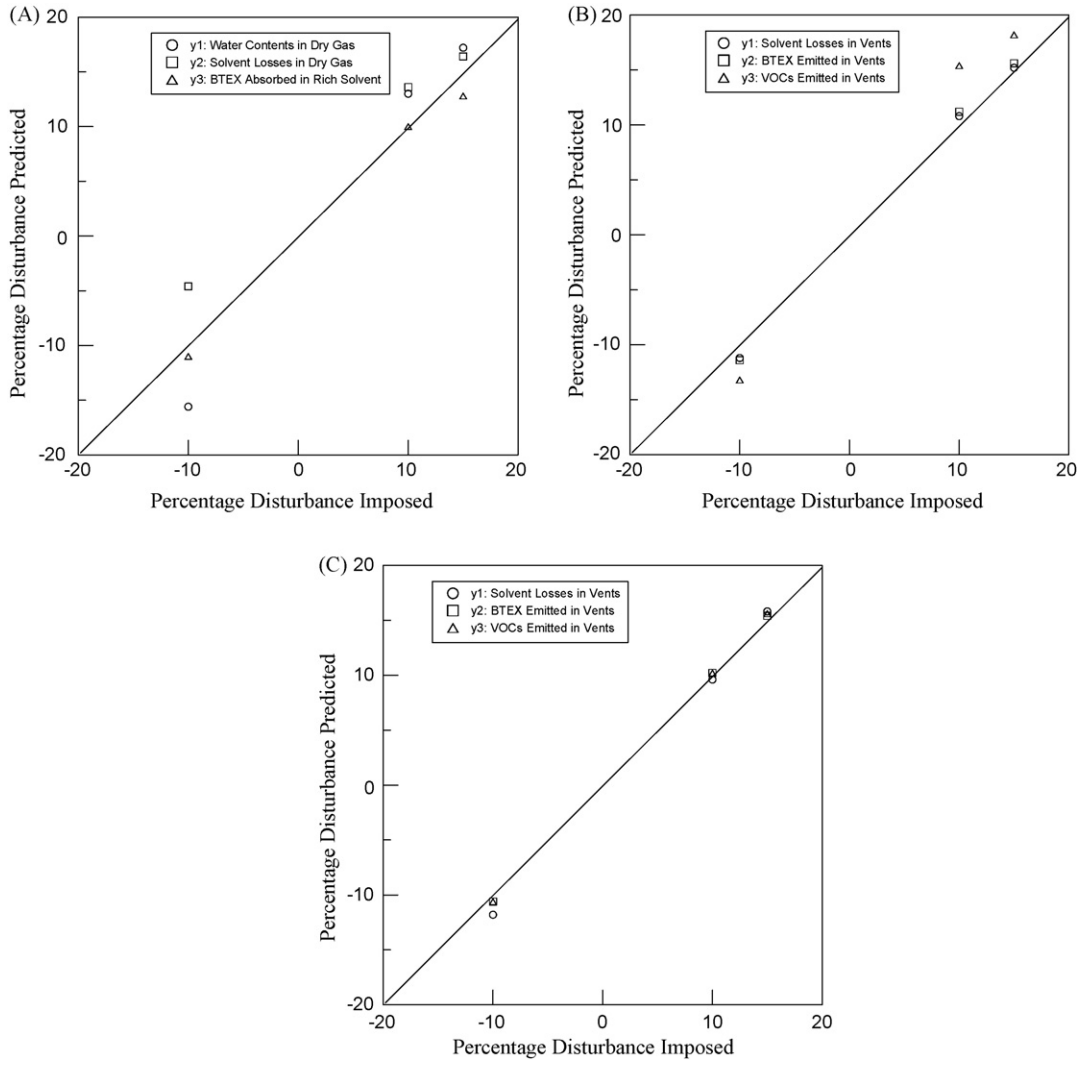

Fig. 6. Faults recall by the ANN trained with "trainoss" algorithm at fault levels of: −5%, +5%, +20%, and −20% (A: contactor, B: stripper–regenerator, C: overall plant).

3. Conclusions

A typical natural gas dehydration plant, which employs triethylene glycol (TEG) as the dehydrating agent, has been simulated using a steady state flowsheet simulator (Aspen Plus). The base case operating conditions are taken to resemble field data from one of the existing dehydration units operating in the United Arab Emirates (UAE). The dew point (water contents) of the dry gas issuing from the contactor is mostly responsive to disturbances in the wet gas flow rate and to a lesser extent to lean solvent circulation rate and water contents in the processed gas. TEG losses are mostly sensitive to the contactor pressure. The temperature of the inlet rich solvent and the stripping gas flow rate profoundly affects BTEX and VOCs emissions, respectively. The most important variable in deciding solvent losses and BTEX emissions from the overall plant is shown to be the circulation rate of the solvent. The higher the circulation rate, the higher are the solvent losses and the BTEX emissions. ANN successfully reflects the disturbance severity levels in the input variables considered for the contactor. In particular, abnormal levels of BTEX concentrations in the rich solvent (exiting the contactor) are shown to precisely indicate the severity levels in these input variables. Faults in the stripper–regenerator unit have been perfectly predicted by the ANN for two symptoms (TEG emissions and BTEX emissions in vents) and to a lesser extent for faults in VOCs emissions. The best ANN prediction is obtained for the overall plant where the ANN perfectly mimics the imposed disturbances for the three severity levels of imposed malfunctions for all symptoms considered.

References

[1] J.M. Campbell, Gas Conditioning and Processing, Volume 2: The Equipment Modules, Campbell Petroleum Series, Norman, Oklahoma, 1992.
[2] F.S. Manning, R.E. Thompson, Oilfield Processing of Petroleum, Volume One: Natural Gas, Pennwell Publishing Company, Tulsa, Oklahoma, 1991.
[3] R.L. Pearce, C.R. Sivalls, Fundamentals of gas dehydration, design and operation with glycol solutions, in: Gas Conditioning Conference, University of Oklahoma, Norman, Oklahoma, 1984.
[4] P.L. Grizzle, Glycol-Reboiler Emissions-2: glycol mass-balance method for estimating scores high for estimating BTEX, VOC emissions, Oil Gas J. 91 (May (22)) (1993) 61.

[5] A.M. Break, R.A. Almehaideb, N. Darwish, R. Hughes, Optimization of process parameters for glycol unit to mitigate the emission of BTEX/VOCs, Trans. IChem. 79 (Part B) (2001) 218–232.
[6] D.B. Robinson, C.-J. Chen, H.-J. Ng, The Solubility of Selected Aromatic Hydrocarbons in TEG, Gas Processing Association, 1991.
[7] C.W. Fitz, R.A. Hubbard, Quick manual calculation estimates amounts of benzene absorbed in glycol dehydrator, Oil Gas J. (November) (1987) 72–75.
[8] D.L. Gallup, E.G. Isacoff, D.N. Smith, Use of ambersorb carbonaceous adsorbent for removal of BTEX compounds from oil-field produced water, Environ. Prog. 15 (Fall (3)) (1996) 197.
[9] C.O. Rueter, M.C. Murff, C.M. Beitler, Glycol Dehydration Operations, Environmental Regulations, and Waste Stream Survey, Gas Research Institute (Environment & Safety Research Group), June 1996.
[10] Title III, Section 112 of 1990 Clean Air Act Amendments.
[11] S. Coerr, New air regulatory requirements for gas processing facilities, in: Seventy-Fourth Gas Processing Association Annual Convention, 1995, p. 188.
[12] C.O. Rueter, J.M. Evans, Impacts of the clean air act amendments on the oil and gas production industry, in: Laurance Reid Gas Conditioning Conference, Norman, Oklahoma, 1995.
[13] J. Collie, M. Hlavinka, A. Ashworth, An analysis of BTEX emissions from amine sweetening and glycol dehydration facilities, in: Laurance Reid Gas Conditioning Conference, Norman, Oklahoma, 1998.
[14] G.W. Sams, Emission control for glycol dehydration equipment, in: Laurance Reid Gas Conditioning Conference, Oklahoma City, Oklahoma, 1990.
[15] D.G. Colley, W.Y. Svreck, H. Adam, Energy and emission optimization of the glycol dehydrator process, in: GRI Glycol Dehydrator Air Emission Conference, New Orleans, Louisina, July, 1992.
[16] N.A. Darwish, R.A. Almehaideb, A.M. Break, Computer simulation of BTEX emission in natural gas dehydration using PR and RKS equations of state with different predictive mixing rules, Environ. Software 19 (2004) 957–965.
[17] S.J. Russell, P. Norvig, Artificial Intelligence-A Modem Approach, Prentice Hall, NJ, 1995.
[18] J. Hertz, A. Krogh, R. Palmer, Introduction to The Theory of Neural Computation, Addison Weslye, Redwood City, California, 1991.
[19] A.B. Bulsari (Ed.), Neural Networks for Chemical Engineers, Elsevier, Amsterdam, 1995.
[20] J.M. Serra, A. Corma, E. Argente, S. Valero, V. Botti, Appl. Catal. 254 (2003) 133.
[21] S.S. Tambe, B.D. Kulkarni, P.B., Deshpande, Elements of Artificial Neural Networks with Selected Applications in Chemical Engineering, and Chemical and Biological Sciences, Simulation and Advanced Controls Ltd., Louisville-KY, U.S.A.
[22] R. Sharma, K. Singh, D. Singhal, R. Ghosh, Neural network applications for detecting process faults in packed towers, Chem. Eng. Process. 43 (7) (2004) 841–847.
[23] V. Venkatasubramanian, K. Chan, A neural network methodology for process fault diagnosis, AIChE J. 35 (1989) 1993–2002.
[24] V. Venkatasubramanian, R. Vaidyanathan, Y. Yamamoto, Process fault detection and diagnosis using neural networks. 1. steady state processes, Comput. Chem. Eng. 14 (7) (1990) 699–712.
[25] D.M. Himmelblau, Fault Diagnosis in Chemical and Petrochemical Processes, Elsevier, Amsterdam, 1978.
[26] T. Sorsa, H.N. Koivo, Application of artificial neural networks in process fault diagnosis, Automatica 29 (4) (1993) 843–849.
[27] K. Watanabe, I. Matsuura, M. Abe, M. Kubota, D.M. Himmelblau, Incipient fault diagnosis of chemical processes via artificial neural networks, J. AIChE 35 (11) (1989) 1803–1812.
[28] F.S. Mjalli, Neural network model-based predictive control of liquid-liquid extraction contactors, Chem. Eng. Sci. 60 (2005) 239–253.
[29] C.M. Bishop, Neural Networks for Pattern Recognition, Oxford Clarendon Press, 1996, p. XVII.
[30] B.D. Ripley, Pattern Recognition and Neural Networks, Cambridge University Press, 1996.
[31] V. Uraikul, C.W. Chan, P. Tontiwachwuthikul, Artificial intelligence for monitoring and supervisory control of process systems', Eng. Appl. Artif. Intelligence 20 (2) (2007) 115–131.
[32] R. Srinivasan, C. Wang, W.K. Ho, K.W. Lim, Context-based recognition of process states using neural networks, Chem. Eng. Sci. 60 (4) (2005) 935–949.